Pergamon

Geochimica et Cosmochimica Acta, Vol. 66, No. 18, pp. 3281–3291, 2002

0016-7037/02 $22.00 + .00

PII S0016-7037(00)00925-0

Reaction rates of natural orpiment oxidation at 25 to 40°C and pH 6.8 to 8.2 and comparison with amorphous As_2S_3 oxidation

MAGGY F. LENGKE[1] and REGINA N. TEMPEL[2,*]

[1]Graduate Program of Hydrologic Sciences, University of Nevada, Reno, NV 89557, USA
[2]Department of Geological Sciences, MS 172, Mackay School of Mines, University of Nevada, Reno, NV 89557, USA

(*Received July* 16, 2001; *accepted in revised form March* 27, 2002)

Abstract—The oxidation rate of natural orpiment from Carlin-type deposits was measured at 25 to 40°C in a mixed flow reactor as a function of pH (6.8 to 8.2) and dissolved oxygen concentration (6.4 to 17.4 ppm) with a starting ionic strength of 0.01 M NaCl. All experiments ran for approximately 30 h, where steady-state conditions were reached after 20 h at a flow rate of 10 mL/min. The stoichiometric ratio of As/S was observed once steady state was reached. The rate law of orpiment oxidation is as follows:

$$R = 10^{-11.77(\pm 0.36)}[\mathrm{DO}]^{0.36(\pm 0.09)}[\mathrm{H}^+]^{-0.47(\pm 0.05)},$$

where R signifies the rate of orpiment destruction (mol m^{-2} s^{-1}), [DO] is the concentration of dissolved oxygen (M), and $[H^+]$ is the concentration of proton (M). The activation energy for the orpiment oxidation by dissolved oxygen at a temperature range of 25 to 40°C is 59.1 kJ/mol. Oxidation reactions of orpiment show incomplete oxidation of arsenic and sulfide in solution. At a pH range of 6.8 to 8.2, As(III) exists as H_3AsO_3 and As(V) is present as $HAsO_4^{2-}$ and $H_2AsO_4^-$. Sulfite, sulfate, and thiosulfate are present as small fractions of total sulfur. The possible major sulfur species are intermediate oxidation state species. The oxidation rate of natural orpiment oxidation is slightly lower by a factor of 0.002 to 0.560 than that of As_2S_3(am) at the considered pH 7 to 10 and DO concentrations of 1 to 10 ppm. The dependence factors on pH for natural orpiment oxidation are lower by a factor of 0.37 compared with As_2S_3(am). However, the calculated activation energy is much larger for natural orpiment than As_2S_3(am) by a factor of 3.5. As(III) and As(V) are the major products for both As_2S_3(am) and natural orpiment oxidation along with intermediate sulfur species. The rate of orpiment oxidation increases with pH and results in an increase in the release of As. In mining-impacted environments with alkaline waters, as may be found in carbonate-hosted ore deposits, the natural attenuation of As oxyanions by sorption to oxide/hydroxide mineral surfaces is minimized because of a negative surface charge at a higher pH range. Thus, As concentrations may increase in mining-impacted waters at higher pH values (>8). *Copyright © 2002 Elsevier Science Ltd*

1. INTRODUCTION

Orpiment (As_2S_3) commonly occurs in hydrothermal and geothermal environments—for example, in Carlin-type gold deposits or hydrothermal disseminated replacement gold deposits (Bonham, 1985). Abundant orpiment is found in Getchell, Nevada, and Mercur, Utah. In other areas, such as Northumberland and Alligator Ridge, Nevada, small amounts of orpiment are present (Bonham, 1985). Orpiment is a reliable mineralogical indicator of gold mineralization in the Enfield Bell Mine and Jerritt Canyon, Elko County, Nevada (Birak and Hawkins, 1985). In other parts of the world, such as in Yugoslavia, Bosnia, Macedonia, Czechoslovakia, Iran, Turkey, the USSR, China, Peru, and Indonesia, orpiment occurs in massive form or with disseminated gold (Anthony et al., 1990; Turner et al., 1994). Orpiment also occurs as a volcanic sublimation product, as a deposit from hot springs, and as an oxidation product of realgar (Boyle and Jonasson, 1972; Birak and Hawkins, 1985; Klein and Hurlbut, 1993).

Minor elements are present in orpiment as structural impurities including mercury (Hg) and antimony (Sb) (Dickson et al., 1975). Thus, the oxidation or weathering of orpiment releases these minor elements in addition to arsenic (As) to the environment and release of these potentially toxic elements may influence the water quality in any area where orpiment is present.

Although As, Hg, and Sb pollution from mine waste dumps have posed a potentially serious environmental problem for decades, the reaction rates involved in the weathering and oxidation reactions of orpiment have not been established before this study.

Only a very few studies have investigated orpiment or As_2S_3(am) oxidation (Ehrlich, 1963; Lazaro et al., 1997; Lengke and Tempel, 2001). Our previous study of As_2S_3(am) oxidation shows that oxygen content and pH significantly influence oxidation rates. Activation energy for As_2S_3(am) oxidation is approximately 16 to 17 kJ/mol. Arsenic (III), As(V), and intermediate sulfur were present as dominant species during the As_2S_3(am) oxidation. Because of the relatively widespread occurrence of natural orpiment, an understanding of natural orpiment oxidation is also important. Thus, the purpose of this study was to measure the oxidation rates of natural orpiment in carbonate solutions and determine the dominant factors controlling the rates. A carbonate solution was chosen because natural orpiment is commonly disseminated in, or

* Author to whom correspondence should be addressed (gina@mines.unr.edu).

Table 1. Summary of experimental conditions and results of orpiment oxidation[a].

					Input			Steady state								
Experiment	Flow Rate (dm^3s^{-1})	Temp (C)	Mass (g)	Time (min)	pH	DO (ppm)	Eh (V)	pH	DO (ppm)	Eh (V)	mAs (mM)	mS (mM)	Saf (m^2g^{-1})	R_{As} (mol $m^{-2}s^{-1}$)	R_s (mol $m^{-2}s^{-1}$)	Error R_{As} (%)	Error R_s (%)
A	1.67×10^{-4}	25	2.106	1725	8.04	7.06	0.222	7.53	6.84	0.123	0.024	0.037	3.56	2.71×10^{-10}	2.75×10^{-10}	22	6
B	1.67×10^{-4}	30	5.013	1780	7.90	6.37	0.221	7.45	5.20	0.123	0.075	0.116	3.73	3.34×10^{-10}	3.46×10^{-10}	22	6
C	1.67×10^{-4}	25	5.022	1735	8.04	7.01	0.227	7.52	6.84	0.126	0.046	0.069	3.25	2.36×10^{-10}	2.34×10^{-10}	22	6
D	1.67×10^{-4}	40	5.160	1735	7.99	5.44	0.219	7.22	4.56	0.133	0.088	0.126	2.86	4.96×10^{-10}	4.77×10^{-10}	22	6
E	1.67×10^{-4}	25	5.244	1745	7.21	7.00	0.258	6.79	6.88	0.128	0.027	0.041	3.12	1.37×10^{-10}	1.41×10^{-10}	22	6
F	1.67×10^{-4}	25	5.140	1815	8.93	7.01	0.208	8.23	6.57	0.083	0.125	0.194	2.92	6.94×10^{-10}	7.2×10^{-10}	22	6
G	1.67×10^{-4}	25	5.270	1725	7.92	7.01	0.317	7.44	6.64	0.153	0.047	0.070	3.28	2.27×10^{-10}	2.27×10^{-10}	22	6
H	1.67×10^{-4}	25	5.140	1695	7.90	7.08	0.268	7.37	6.91	0.146	0.055	0.083	3.25	2.76×10^{-10}	2.78×10^{-10}	22	6
J	1.67×10^{-4}	25	5.075	1650	8.02	15.94	0.277	7.33	14.73	0.167	0.045	0.067	2.32	3.17×10^{-10}	3.16×10^{-10}	22	6
AA	1.67×10^{-4}	30	4.898	1665	8.02	6.37	0.297	7.42	5.18	0.091	0.051	0.078	3.35	2.62×10^{-10}	2.63×10^{-10}	22	6
BB	1.67×10^{-4}	40	4.985	1385	8.00	5.44	0.246	7.39	4.51	0.088	0.098	0.136	2.86	5.75×10^{-10}	5.31×10^{-10}	22	6
DD	1.67×10^{-4}	25	5.007	1710	7.26	7.00	0.290	6.86	6.72	0.090	0.024	0.036	2.32	1.71×10^{-10}	1.72×10^{-10}	22	6
EE	1.67×10^{-4}	25	5.022	1720	7.90	19.63	0.303	7.57	17.42	0.119	0.068	0.104	3.12	3.63×10^{-10}	3.70×10^{-10}	22	6
EEE	1.67×10^{-4}	25	5.020	1720	7.89	19.50	0.302	7.49	17.39	0.118	0.067	0.099	3.12	3.56×10^{-10}	3.52×10^{-10}	22	6
FF	1.67×10^{-4}	25	5.010	1710	8.88	7.05	0.260	8.24	6.37	0.082	0.121	0.186	2.92	6.91×10^{-10}	7.08×10^{-10}	22	6

[a] Saf is final surface area. Initial surface area of all experiments is 2.88 m^2/g.

surrounded by, carbonate rocks—for example Carlin-type deposits (Bonham, 1985; Shevenell et al., 1999). The majority of the sampled mine waters from the Carlin-type deposits in Nevada had pH values between 6.5 and 8.5 (Shevenell et al., 1999). Thus, in this study, the geochemical parameters investigated were limited to pH (6.8 to 8.2), dissolved oxygen (6.4 to 17.4 ppm), and temperature (25 to 40°C).

2. MATERIALS AND METHODS

2.1. Characterization and Pretreatment of the Solid

Natural orpiment samples used in this study were obtained from Carlin-type deposits of the Getchell Mine, Humboldt County, Nevada. The samples were hand-sorted to remove macroscopic impurities, crushed in a steel mortar, and sieved to a size fraction between 44 and 74 μm. After sieving, the sample was cleaned with ethanol and repeatedly shaken to remove fine particles adhering to the surface. This procedure was repeated a dozen times until the supernatant was relatively clear and was followed by wet sieving through nylon sieves. An ultrasonic cleaning was not applied in this study because of the tendency of the mineral to disintegrate. The sample was dried and then placed in a vacuum desiccator until use.

The sample was examined with a Phillips XRG 3100 X-ray diffractometer to ensure purity and ascertain crystallinity. Standard X-ray diffraction techniques were applied by means of CuK_α radiation generated at 40 kV and 30 mA. The scan was carried out with 2θ values from 10 to 60°. Microscopic analysis of fresh/cleaned and oxidized orpiment samples were performed with a JEOL JSM-840A scanning electron microscope. The composition of the solid was also determined by scanning electron microscope (SEM) equipped with an energy dispersive spectrometer.

Bulk chemical analyses of thirty-four elements for two samples were determined by aqua regia digestion (HNO_3/HCl) followed by inductively coupled plasma mass spectrometry (ICP-MS), and these results were then averaged. The samples contain relatively high concentrations of Sb (17509 ppm), Hg (60 ppm), and selenium (Se) (87 ppm). The molar ratio of As/S is ~0.68 ± 0.00 on the basis of the bulk chemical analyses of As and S. All ICP-MS analyses were performed by Acme Analytical Laboratory (Vancouver, British Columbia, Canada), and samples were analyzed within a week of the experiments.

Specific surface areas were determined by multipoint fits to a BET isotherm with Kr gas in a Micromeritics ASAP 2405 BET surface area analyzer (Micromeritics Materials Analysis Laboratory). The uncertainty on BET surface area measurements is ± 10%. The measurements of surface area were made on fresh/cleaned and oxidized samples.

2.2. Experimental Methodology

Details of experimental methods including the reactor design, preparation, sampling, preservation, and analysis of output solution are described in Lengke and Tempel (2001). Experiments were conducted to determine the effects of pH, oxygen, and temperature on orpiment oxidation in a mixed flow reactor. Variable oxygen concentrations were prepared by saturating feed solutions with either highly pure oxygen (99.9%) or ambient air. Variable pH values (7.2 to 8.9) in feed solutions were prepared with analytical reagent grade sodium carbonate (Na_2CO_3) and/or sodium bicarbonate ($NaHCO_3$) and distilled, deionized water. Ionic strength of the feed solutions was adjusted to 0.01 mol/L with sodium chloride (NaCl).

An initial orpiment mass of approximately 5 g was used in each experiment and the actual weight is listed in Table 1. The output solution was collected every hour from 0 to 8 h and from 24 to approximately 30 h. The pH, Eh, and DO were continuously monitored with an Orion 420A pH/millivolt-meter and Orion 810 or Orion 862A DO meters. The uncertainties in measured pH and DO are ±0.02 pH units and ±0.05 ppm. All experiments were performed in the dark by wrapping the reactor with aluminum foil. Steady-state conditions were defined by a series of constant As and S output concentrations so that the standard deviation of the output solutions was less than 6%.

Total dissolved As and S were analyzed with an Optima 3000 DV inductively coupled plasma atomic emission spectroscopy (ICP-AES) by Acme Analytical Laboratory within a week. Analytical detection limits for As and S were 30 ppb and 0.1 ppm, respectively, on ICP-AES. The uncertainties in measured As and S concentrations were ±5 and ±2%, respectively, and were determined by analyzing the same sample three times.

Sulfur species including sulfate (SO_4^{2-}), sulfite (SO_3^{2-}), and thiosulfate ($S_2O_3^{2-}$) were determined with a Dionex EX100 ion chromatography by Huffman Analytical Laboratory. Output solutions for sulfur species were preserved with 0.1 mol/L triethanolamine and frozen until analysis, approximately a week. Analytical detection limits for S species were 0.1 ppm for SO_4^{2-} and 0.3 ppm for SO_3^{2-} and $S_2O_3^{2-}$ with ±0.1 ppm for SO_4^{2-} and ± 0.3ppm for SO_3^{2-} and $S_2O_3^{2-}$.

As(III) and total As were determined with hydride generation coupled with a Varian Spectra 220 atomic absorption spectrometer (AA). The output solutions for arsenic species were stored in amber polyethylene bottles and were frozen until analysis without chemical preservative, approximately within a week. The standard solutions for As(III) were prepared in ascorbic acid (1 mol/L) as a preservative agent,

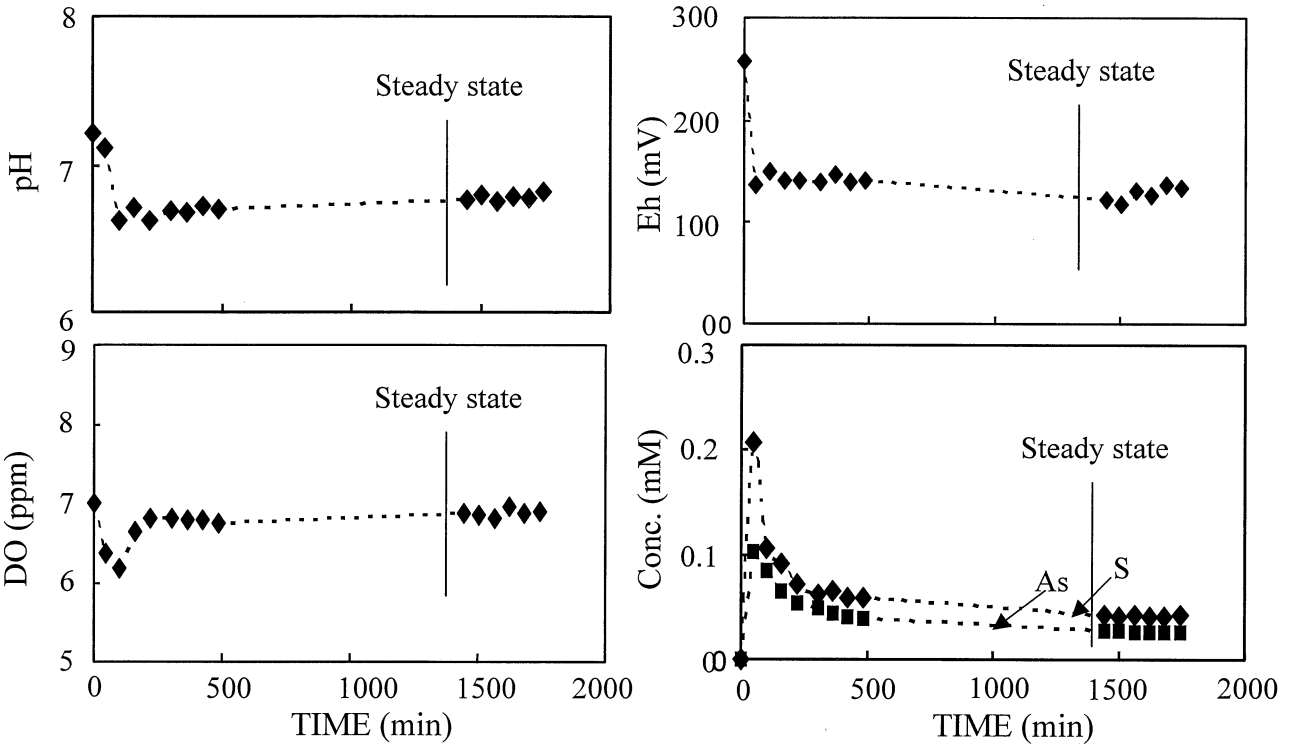

Fig. 1. Representative changes in DO, pH, Eh, As, and S as a function of time until steady-state conditions are achieved (shown for experiment E).

whereas the standard solutions for total As were prepared in hydrochloric acid (0.01 mol/L). As(V) was calculated by subtracting the As(III) from the total As determined on an aliquot of the sample. The uncertainty in measured As(III) and total As was ±5%. The results of total As from AA and ICP-AES were similar.

2.3. Calculation of Reaction Rates and Uncertainties

Steady-state oxidation rates in a mixed flow reactor were determined with the following expression (Levenspiel, 1972):

$$R_{\text{min}} = \frac{(C_{\text{out}} - C_{\text{in}})\text{q}}{v_i A_{\text{min}}}, \tag{1}$$

where C_{out} and C_{in} are the output and feed solutions (M), respectively, v_i is the stoichiometric coefficient of i in the mineral formula, q is the flow rate through the system (L s^{-1}), and A_{min} is the total surface area (m^2).

The error (ε) in the calculated rate is estimated with the error propagation method (Barrante, 1998) by the following equation:

$$(\varepsilon(R)^2) = \left(\frac{C}{A}\right)^2 \times (\varepsilon(q))^2 + \left(\frac{q \times C}{A^2}\right)^2 \times (\varepsilon(A))^2 + \left(\frac{q}{A}\right) \times (\varepsilon(C))^2 \tag{2}$$

where R is the oxidation rate, C is the output concentration, q is the flow rate, and A is the mineral surface area.

3. RESULTS

3.1. Mixed Flow Experiments

All experiments ran for approximately 30 h, and the experimental results are compiled in Table 1. The steady-state oxidation rates in this study were derived from the data points collected close to the end of each experiment or after 20 h at a flow rate of 10 mL/min. For each experiment, six data points or more at steady-state conditions were collected. An example of steady-state conditions is shown in Figure 1.

The oxidation rates of orpiment were normalized to final surface areas. The calculated total dissolved material, based on output concentrations of As and S, was less than 6% of the orpiment starting material. Because the percentage of mass dissolved in any experiment was low, any change in total surface area resulting from the oxidation reaction was probably small. However, significant changes in measured final surface areas for some samples were observed (e.g., experiment B) and these differences may be due to uncertainty in surface area measurements (±10%) and/or mechanical disaggregation/aggregation during the duration of the experiments. If the surface area were continually changing as a function of time throughout an experiment, we would not expect to achieve steady-state reaction behavior (Nagy and Lasaga, 1992). However, all the measured rates reached steady state after 20 h and remained at steady state until 30 h.

Uncertainties in the measured oxidation rates arise from the measurement of solution concentrations, fluid flow rates, and mineral surface areas. Uncertainties in the solution concentrations are ±5% and ±2% for As and S, respectively. Uncertainties in fluid flow rate are ≤1%. The error in the calculated oxidation rates from Eqn. 2 ranges from 6 to 22% and is influenced mostly by the BET surface area measurement (±10%).

Table 2. Summary of sulfur species.

Experiment	$mS_{(T)}$ (mM)	mSO_4^{2-} (mM)	mSO_4^{2-} (%)	$mS_2O_3^{2-}$ (mM)	$mS_2O_3^{2-}$ (%)	mSO_3^{2-} (mM)	mSO_3^{2-} (%)	Other S (mM)	Other S (%)
B	0.116	0.006	5.38	<0.003	—	0.004	3.23	0.106	91.39
C	0.069	0.006	9.10	<0.003	—	<0.004	—	0.062	90.90
D	0.126	0.008	6.59	0.003	2.12	0.004	3.46	0.111	87.83
E	0.041	0.005	12.58	0.003	7.55	<0.004	—	0.033	79.87
F	0.194	0.016	8.33	0.013	6.91	0.006	3.23	0.158	81.53
G	0.070	0.007	10.38	0.006	8.90	<0.004	—	0.057	80.73
J	0.067	0.003	4.67	0.004	6.01	0.004	6.54	0.055	82.78
AA	0.078	0.004	5.38	<0.003	—	<0.004	—	0.073	94.62
BB	0.136	0.005	3.83	0.004	3.28	0.007	5.06	0.119	87.83
CC	0.081	0.005	6.41	<0.003	—	0.004	4.62	0.072	88.97
DD	0.036	0.004	11.59	<0.003	—	<0.004	—	0.032	88.41
EE	0.104	0.004	4.00	<0.003	—	<0.004	—	0.100	96.00
FF	0.186	0.016	8.70	0.013	7.22	0.006	3.37	0.150	80.72

3.2. Sulfur and Arsenic Species

Sulfur oxyanions, in the pH range of 6.8 to 8.2 at 25 to 40°C, are produced as intermediates during orpiment oxidation (Table 2). The results show that the measured sulfate, sulfite, and thiosulfate constitute only a small fraction of total S (<2 to 12.6%). Other sulfur intermediates that may include polythionates constitute 81 to 96% of total S.

Arsenic (III) is present with As(V) and constitutes approximately 51 to 68.5% of the total As in the pH range of 6.8 to 8.2 (Table 3). The ratio of As(III)/As(V) is ~1.1 to 2.2, regardless of the total As concentrations.

4. DISCUSSION

The measured ratios of total As/S in steady-state conditions (0.64 to 0.72) are very close to stoichiometric ratios, considering the uncertainty of total As and S measurements by ICP-AES. The stoichiometric relationship between As and S concentrations are represented by a plot of log oxidation rates that were obtained on the basis of the release of As vs. those that were obtained on the basis of the release of S, as shown in Figure 2. The nearly stoichiometric ratios suggest the lack of secondary mineral precipitation.

Further evidence that mineralogical composition remained uniform during experiments was observed by X-ray diffraction analysis of oxidized and fresh/cleaned orpiment and SEM photomicrographs of the surface of oxidized orpiment (Fig. 3). There are always small particles adhering to the surface after oxidation experiments. However, no alteration on the surface has been observed, indicating the absence of secondary precipitation. Additionally, outlet solutions were undersaturated, on the basis of theoretical geochemical modeling calculations, with respect to all possible secondary phases in all experiments. Mineral saturation states were computed by PHREEQC (Parkhurst and Appelo, 1999).

4.1. Variable Dissolved Oxygen Concentrations and pH

Steady-state orpiment oxidation at pH ~7.5 and 25°C is illustrated as a function of DO (6.6 to 17.4 ppm) in Figure 4. The data used are tabulated in Table 1 (experiments A, C, H, J, EE, and EEE). The linear curve of a plot of log oxidation rate vs. log DO yields a slope of 0.36 ± 0.09, and the coefficient of determination (R^2) of the data fit is 0.81. This result indicates that the rate of orpiment oxidation is dependent on the concentration of dissolved oxygen content within the range of oxygen concentrations used in this study.

The measured steady-state data of orpiment oxidation rates at 25°C and at the pH range of 6.8 to 8.2 are shown in Table 1 (experiments A, C, E, F, G, H, DD, and FF) and illustrated in

Table 3. Summary of As species.

Experiment	As(T) (M)	As(III) (M)	As(III) (%)	As(V) (M)	As(V) (%)
A	2.43×10^{-5}	1.45×10^{-5}	59.72	9.79×10^{-6}	40.28
B	7.47×10^{-5}	4.07×10^{-5}	54.55	3.39×10^{-5}	45.45
C	4.60×10^{-5}	2.42×10^{-5}	52.65	2.18×10^{-5}	47.35
D	8.76×10^{-5}	5.51×10^{-5}	62.88	3.25×10^{-5}	37.12
E	2.68×10^{-5}	1.65×10^{-5}	61.63	1.03×10^{-5}	38.37
F	1.25×10^{-4}	7.04×10^{-5}	56.54	5.41×10^{-5}	43.46
G	4.68×10^{-5}	2.89×10^{-5}	61.77	1.79×10^{-5}	38.23
H	5.51×10^{-5}	3.40×10^{-5}	61.81	2.10×10^{-5}	38.19
J	4.46×10^{-5}	2.28×10^{-5}	50.98	2.26×10^{-5}	50.59
AA	5.14×10^{-5}	3.19×10^{-5}	62.00	1.95×10^{-5}	38.00
BB	9.81×10^{-5}	6.29×10^{-5}	64.08	3.53×10^{-5}	36.03
DD	2.38×10^{-5}	1.63×10^{-5}	68.49	7.51×10^{-6}	31.51
EE	6.80×10^{-5}	3.58×10^{-5}	52.65	3.30×10^{-5}	48.53
FF	1.21×10^{-5}	7.05×10^{-5}	58.36	5.03×10^{-5}	41.64

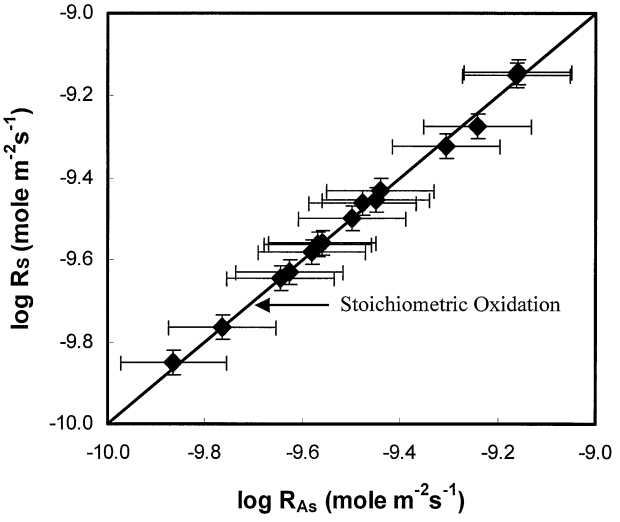

Fig. 2. Comparison of the orpiment oxidation rates that were obtained on the basis of the release of As to those obtained on the basis of the release of S at various conditions.

Figure 5. The pH values are plotted against log rate and (log rate − n log DO). Both linear curves represent least squares fits of the data and yield similar slopes of 0.47 ± 0.05. The coefficient of determination (R^2) of the fit for both curves is 0.94. The plot indicates that natural orpiment oxidation rates increase at higher pH values.

4.2. Rate Laws

Within experimental uncertainty, the orpiment oxidation rates, measured at 25°C, can be represented by the rate law:

$$R = 10^{-11.77(\pm 0.36)}[\mathrm{DO}]^{0.36(\pm 0.09)}[\mathrm{H}^+]^{-0.47(\pm 0.05)} \quad (3)$$

where R is the rate of orpiment destruction (mol m^{-2} s^{-1}), [DO] is the concentration of dissolved oxygen (M), and [H^+] is the concentration of proton (M).

The orpiment oxidation rates were measured at 25, 30, and 40°C at pH ~7.4 (Table 1, experiments A, B, C, D, G, H, AA, and BB). The orpiment oxidation rates increased with increasing temperature (25 to 40°C) twofold. The effect of temperature on the oxidation rates was expressed by the Arrhenius equation, as follows:

$$k = A_{\mathrm{exp}}(-E_a/R\mathrm{T}) \quad (4)$$

where k is the oxidation rate constant, A is a preexponential factor, T is temperature (kelvin), R is the gas constant, and E_a refers to the activation energy. The plot of log rate constant vs. 1000/T (K) yields apparent activation energies of 59.1 ± 0.44 kJ/mol (Fig. 6). The relatively large values of the activation energies for orpiment at pH ~7.4 suggest that the reaction rate is controlled by a surface reaction mechanism (Lasaga, 1998). The preexponential factor that was depicted from the intercept of the plot is 3.4×10^{-2}. By combining Eqns. 3 and 4, the orpiment oxidation rates as a function of DO, pH, and temperature can be described as follows:

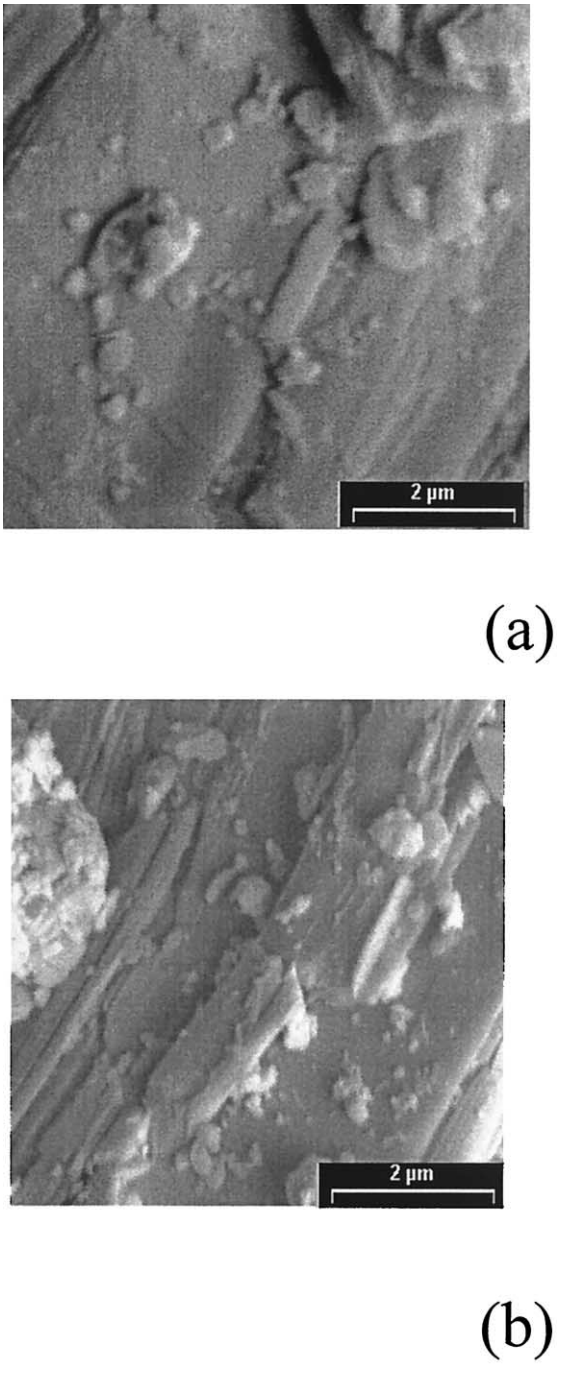

Fig. 3. SEM photomicrographs of (a) unreacted, cleaned orpiment and (b) oxidized orpiment after ~30 h (experiment E). Both unreacted and oxidized surfaces show a similar appearance, with small particles adhering to the surfaces. The oxidized surfaces show no changes in mineralogical composition and no extensive pitting.

$$R = A_{\mathrm{exp}}(-E_a/R\mathrm{T})[DO]^{0.36}[H^+]^{-0.47} \quad (5)$$

where E_a = 59.1 kJ/mol and $A = 3.4 \times 10^{-2}$ mol m^{-2} s^{-1}.

Orpiment oxidation rates were calculated for a range in pH (6 to 9) and DO values (1 to 9 ppm) at 25°C by means of Eqn. 3, and assuming that the rate law remains constant. The orpi-

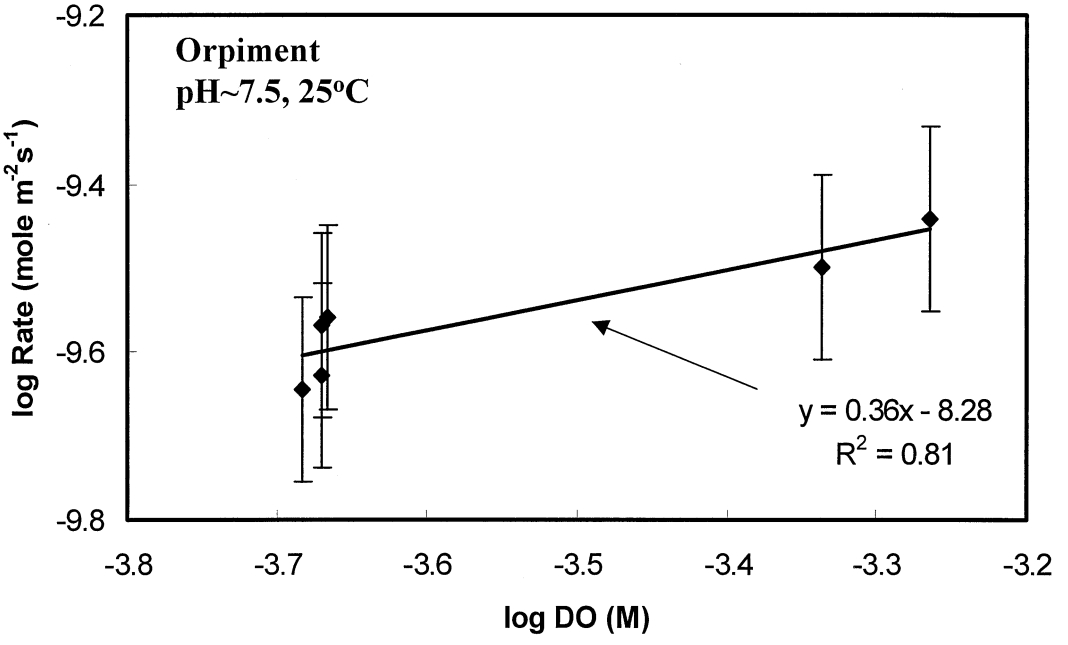

Fig. 4. Effect of dissolved oxygen (DO) on the oxidation rate of natural orpiment at pH ~7.5 and 25°C. The dependence factor of orpiment oxidation on DO is 0.36 ± 0.09, and R^2 is 0.81.

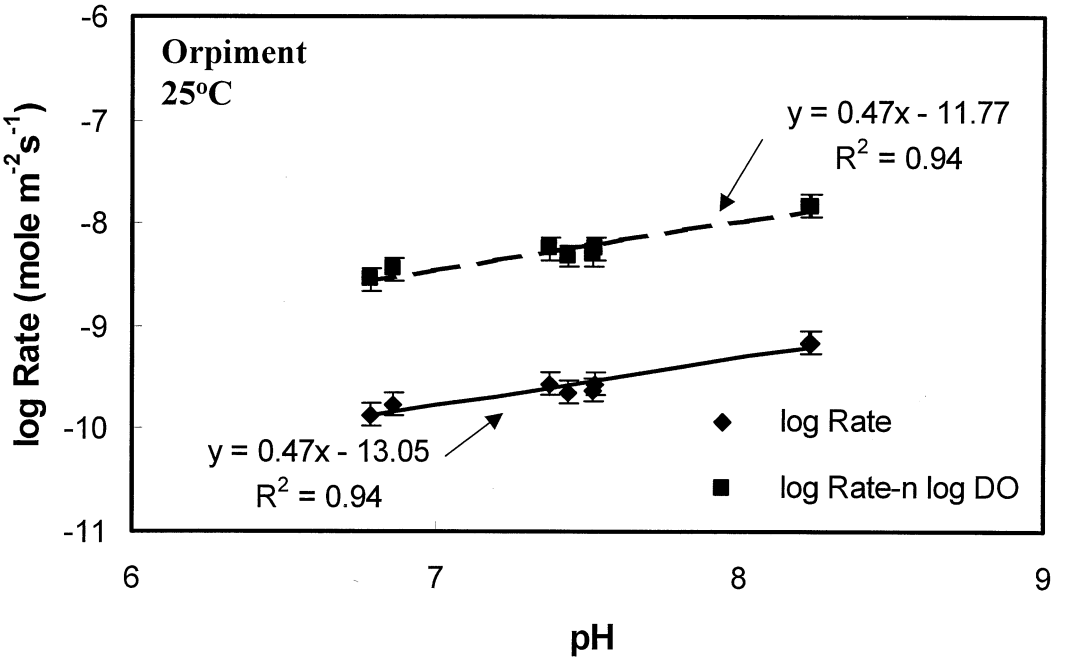

Fig. 5. Effect of pH on the oxidation rate of orpiment at 25°C. The straight line is the linear plot of log oxidation rate vs. pH and the dotted line is the linear plot of log oxidation rate − n log(DO) vs. pH. Both linear curves yield similar dependency factors of 0.47 ± 0.05 and R^2 of 0.94.

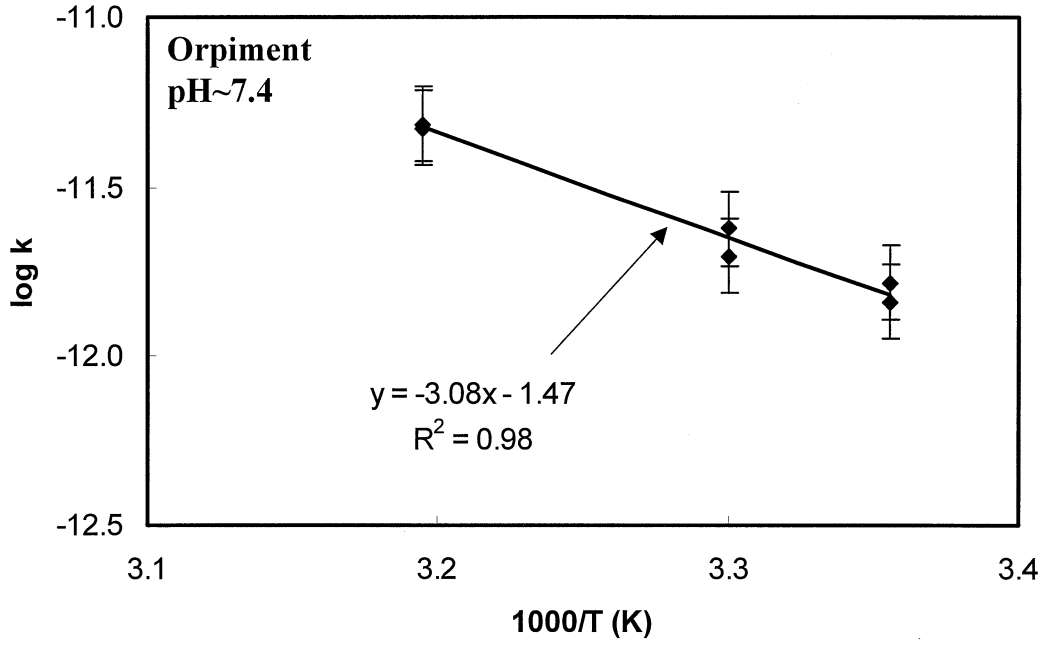

Fig. 6. Arrhenius plots for the oxidation rate constants of orpiment at 25, 30, and 40°C. The plot yields a slope of −3.08 ± 0.23 and R^2 of 0.98.

ment oxidation rates increase monotonically with increasing pH at different concentrations of DO, as shown in Figure 7. The oxidation rates of orpiment increase approximately 1.5 times from pH 6 to 9 at a constant DO concentration, and an approximately half order of magnitude from DO concentrations of 1 to 9 ppm at a constant pH. The plot may be used to predict the effects that variable environmental conditions may exert on the oxidation rate of orpiment, assuming that the same rate law applies throughout the considered range of pH and DO values.

4.3. Sulfur and Arsenic Species

Intermediate sulfur oxyanions are present during orpiment oxidation (Table 2) and sulfur species other than sulfate, sulfite, and thiosulfate are the dominant products and were not assessed further in this study. The other possible sulfur species produced during orpiment oxidation are aqueous sulfur with intermediate oxidation states that persist in metastable state in solutions. Sulfide is known to occur in anoxic environments

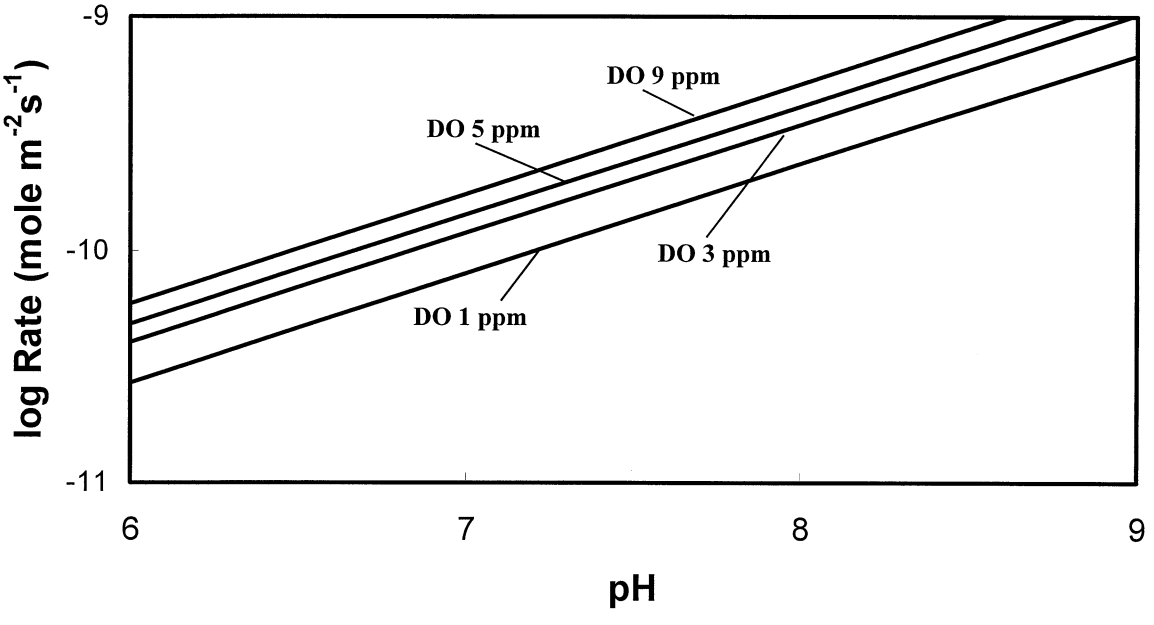

Fig. 7. Predicted orpiment oxidation rates as a function of pH at temperature of 25°C and DO concentration of 1 to 9 ppm by Eqn. 3 (log rate = −11.77 + 0.36 log(DO) + 0.47 pH).

where the rate of oxygen removal is close to or exceeds its rate of supply (Al-Farawati and van den Berg, 1999). This study was conducted in an oxic environment; thus, sulfide may not be important. Polythionates may be present during orpiment oxidation because polythionates occur during pyrite oxidation at low to high pH values (Goldhaber, 1983; McKibben and Barnes, 1986; Moses et al., 1987). Goldhaber (1983) found that at pH 6 to 7, tetrathionate and sulfate were the major observed species and at higher pH values (7.5 to 9) polythionates become unstable and thiosulfate and sulfate predominate. McKibben and Barnes (1986) observed minor metastable sulfur oxyanions at pH < 4. Moses et al. (1987) observed metastable sulfur oxyanions in solutions only at high stirring rates. They suggested that this is due to the quick removal of sulfur oxyanions from near the pyrite surface, which acts as a catalyst for their oxidation to sulfate.

The species of As were calculated by the geochemical modeling PHREEQC (Parkhurst and Appelo, 1999) because As speciation by the hydride generation method only gives the valence states of As. At a pH range of 6.8 to 8.2, As(III) exists as H_3AsO_3 (51.6 to 68.5%) as the dominant As(III) species and as less than 6% in the form of $H_2AsO_3^-$ (Table 4). Arsenic (V) is present as $HAsO_4^{2-}$ (20 to 43.5%) and $H_2AsO_4^-$ (1 to 15.6%), as shown in Table 4.

4.4. Orpiment Oxidation Reactions

The reactions of orpiment oxidation by dissolved oxygen as the primary oxidant may be written as follows:

$$As_2S_3 + 10O_2 + 6H_2O \rightarrow 2HAsO_4^{2-} + 3SO_4^{2-} + 10H^+ \quad (6)$$

or

$$As_2S_3 + 10O_2 + 6H_2O \rightarrow 2H_2AsO_4^- + 3SO_4^{2-} + 8H^+ \quad (7)$$

However, our experimental results suggest that orpiment oxidation may not proceed to completion as presented in reactions 6 and 7. Partial oxidation of orpiment by dissolved oxygen produces As(III) in solution and intermediate aqueous sulfur. Incomplete oxidation of orpiment to aqueous H_3AsO_3, the dominant species of As(III) on the basis of geochemical modeling results, is

$$As_2S_3 + 6O_2 + 6H_2O \rightarrow 2H_3AsO_3 + 3SO_4^{2-} + 6H^+ \quad (8)$$

4.5. As_2S_3(am) vs. Natural Orpiment Oxidation

The oxidation of As_2S_3(am) has been discussed at length in Lengke and Tempel (2001). A comparison of our rate laws for both As_2S_3(am) and natural orpiment are shown in Table 5. As_2S_3(am) is found in geothermal environments and hot springs, whereas the presence of natural orpiment is commonly associated with hydrothermal and geothermal ore deposits. The As_2S_3(am) oxidation shows higher dependency on pH than that of orpiment oxidation. The activation energy of natural orpiment oxidation at a similar pH value and temperature range is much larger than that of As_2S_3(am) (Table 5). The magnitude of the activation energy often offers an important clue regarding the reaction mechanism (Lasaga, 1998). For example, diffusion-controlled reactions in solution have low activation energies (<20 kJ/mol), and a higher experimental Ea would

Table 4. Summary of As species and concentrations calculated using PHREEQC.

Experiment	As(T) M	As(III) M	As(III) %	H_3AsO_3 M	H_3AsO_3 %	$H_2AsO_3^-$ M	$H_2AsO_3^-$ %	As(V) M	As(V) %	$HAsO_4^{2-}$ M	$HAsO_4^{2-}$ %	$H_2AsO_4^-$ M	$H_2AsO_4^-$ %
A	2.43×10^{-5}	1.45×10^{-5}	59.72	1.43×10^{-5}	58.49	3.17×10^{-7}	1.30	9.79×10^{-6}	40.28	8.72×10^{-6}	35.90	1.08×10^{-6}	4.45
B	7.47×10^{-5}	4.07×10^{-5}	54.55	3.99×10^{-5}	53.45	8.90×10^{-7}	1.19	3.39×10^{-5}	45.45	2.97×10^{-5}	39.75	4.3×10^{-6}	5.76
C	4.60×10^{-5}	2.42×10^{-5}	52.65	2.38×10^{-5}	51.63	5.17×10^{-7}	1.12	2.18×10^{-5}	47.35	1.94×10^{-5}	42.11	2.45×10^{-6}	5.33
D	8.76×10^{-5}	5.51×10^{-5}	62.88	5.42×10^{-5}	61.83	1.01×10^{-6}	1.15	3.25×10^{-5}	37.12	2.64×10^{-5}	30.14	6.20×10^{-6}	7.08
E	2.68×10^{-5}	1.65×10^{-5}	61.63	1.65×10^{-5}	61.50	6.68×10^{-8}	0.25	1.03×10^{-5}	38.37	6.31×10^{-6}	23.55	4.17×10^{-6}	15.56
F	1.25×10^{-4}	7.04×10^{-5}	56.54	6.34×10^{-5}	50.93	7.01×10^{-6}	5.70	5.41×10^{-5}	43.46	5.29×10^{-5}	42.45	1.30×10^{-6}	1.04
G	4.68×10^{-5}	2.89×10^{-5}	61.77	2.84×10^{-5}	60.77	5.15×10^{-7}	1.10	1.79×10^{-5}	38.23	1.56×10^{-5}	33.33	2.37×10^{-6}	5.06
H	5.51×10^{-5}	3.40×10^{-5}	61.81	3.36×10^{-5}	60.97	5.18×10^{-7}	0.94	2.10×10^{-5}	38.19	1.79×10^{-5}	32.50	3.20×10^{-6}	5.81
J	4.46×10^{-5}	2.28×10^{-5}	50.98	2.25×10^{-5}	50.37	3.16×10^{-7}	0.71	2.26×10^{-5}	49.02	1.89×10^{-5}	42.35	3.71×10^{-6}	8.31
AA	5.14×10^{-5}	3.19×10^{-5}	62.00	3.13×10^{-5}	60.84	6.50×10^{-7}	1.26	1.95×10^{-5}	38.00	1.69×10^{-5}	32.88	2.63×10^{-6}	5.12
BB	9.81×10^{-5}	6.29×10^{-5}	64.08	6.12×10^{-5}	62.36	1.69×10^{-6}	1.72	3.53×10^{-5}	36.03	2.88×10^{-5}	29.36	4.57×10^{-6}	4.66
DD	2.38×10^{-5}	1.63×10^{-5}	68.49	1.63×10^{-5}	68.28	7.75×10^{-8}	0.33	7.51×10^{-6}	31.51	4.76×10^{-6}	19.98	2.76×10^{-6}	11.58
EE	6.80×10^{-5}	3.58×10^{-5}	52.65	3.49×10^{-5}	57.32	8.54×10^{-7}	1.40	3.30×10^{-5}	48.53	2.96×10^{-5}	43.53	3.34×10^{-6}	4.91
FF	1.21×10^{-5}	7.05×10^{-5}	58.36	6.34×10^{-5}	52.45	7.25×10^{-6}	6.00	5.03×10^{-5}	41.64	4.92×10^{-5}	40.73	1.18×10^{-6}	0.98

Table 5. Comparison of experimentally determined rate laws of amorphous As_2S_3(am) and orpiment oxidation.

Study	pH	DO (ppm)	Rate laws (25°C)	T (°C)	Activation energy (kJ/mol)
Present	6.8–8.2	6.4–17.4	$R = 10^{-11.77}[DO]^{0.36}[H^+]^{-0.47}$	25–40	$E = 59.1 \pm 0.44$
Lengke and Tempel (2001)	6.9–7.9	6.7–17.3	$R_{(As)} = 10^{-16.78}[DO]^{0.42}[H^+]^{-1.26}$ $R_{(S)} = 10^{-17.00}[DO]^{-0.35}[H^+]^{-1.25}$	25–40	$E_{(As)} = 16.8 \pm 5.0$ $E_{(S)} = 16.3 \pm 5.4$

indicate a surface reaction mechanism (Lasaga, 1998). On the basis of the magnitude of activation energies, our results suggest that orpiment oxidation is controlled by a chemical surface reaction mechanism and that As_2S_3(am) oxidation may be controlled by diffusion.

The oxidation rate of As_2S_3(am) varies from slightly higher to lower than that of natural orpiment within a factor of 0.002 to 800 times over the considered pH (3 to 10) and DO (1 to 10 ppm) ranges. Thus, the oxidation rates of orpiment differ from those of As_2S_3(am), suggesting that reaction mechanisms for oxidation of the two solids are likely different.

4.6. Implications for Water Quality at Mining-Impacted Sites

Because numerous experimental studies have been carried out to investigate the mechanisms and rates of pyrite oxidation in mining environments (i.e., Goldhaber, 1983; Nicholson et al., 1988, 1990), it is interesting to compare the rates of orpiment to pyrite oxidation. The rate law for pyrite oxidation by dissolved oxygen has been derived by Williamson and Rimstidt (1994) over four orders of magnitudes in DO concentration and pH ranges of 2 to 10 as follows:

$$R = 10^{-8.19(\pm 0.10)}\,[DO]^{0.50(\pm 0.04)}[H^+]^{-0.11(\pm 0.01)}, \quad (9)$$

where R is the oxidation rate (mol m^{-2} s^{-1}), [DO] is the dissolved oxygen content (M), and $[H^+]$ is the proton concentration (M). This rate law was used to compare pyrite oxidation rates to orpiment oxidation rates derived by this study. The comparison of oxidation rates of pyrite vs. those of orpiment is plotted in Figure 8. The plot shows that oxidation rates of pyrite are up to 88 times higher than orpiment from pH 5 to 7 and DO concentrations of 1 to 9 ppm. However, the oxidation rates of pyrite are up to three times lower than orpiment at pH 9 and DO concentrations of 1 to 7 ppm.

The orpiment particle longevity was calculated by assuming a spherical form by using the following equation (Lasaga, 1998):

$$t = \frac{r}{R \times V} \quad (10)$$

where t is lifetime (s), r is initial radius of the grain (cm), R is dissolution or oxidation rate (mol cm^{-2} s^{-1}), and V is molar volume (cm^3/mol). The estimated lifetime of an orpiment particle is also calculated for variable diameter (10^{-3} to 10^3 μm) at pH 7 and DO 7 ppm and shown in Figure 9. Within the

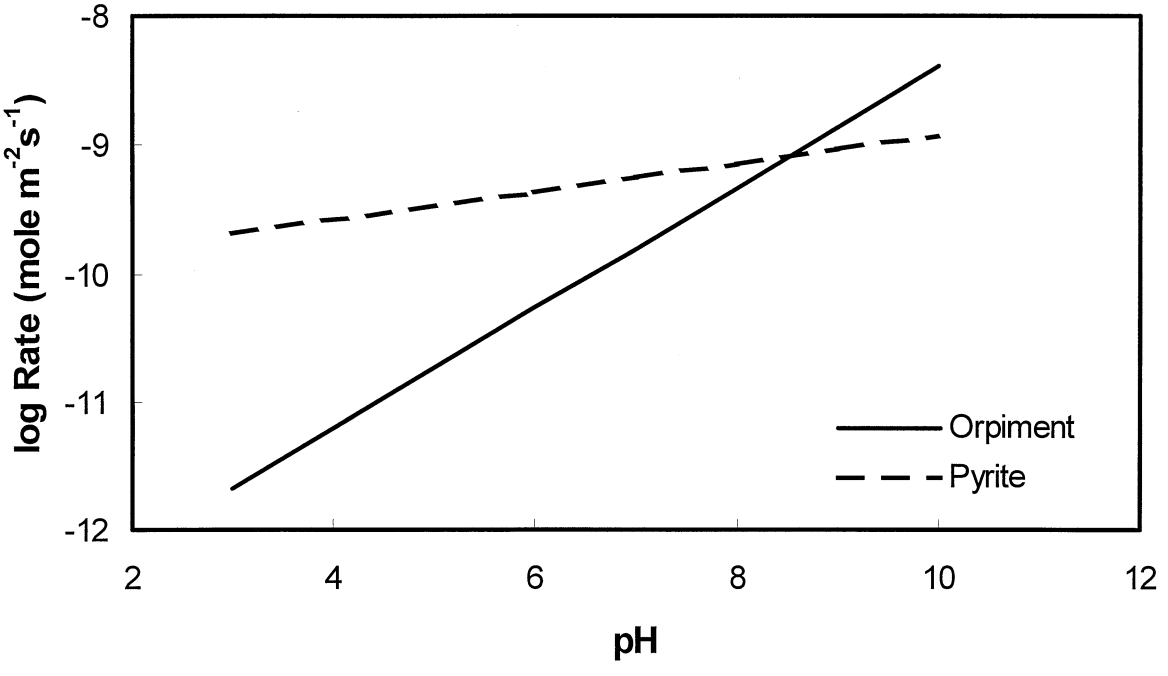

Fig. 8. Comparison of orpiment to pyrite oxidation rates as a function of pH at DO concentration of 7 ppm and temperature 25°C by means of Eqns. (3) and (8)

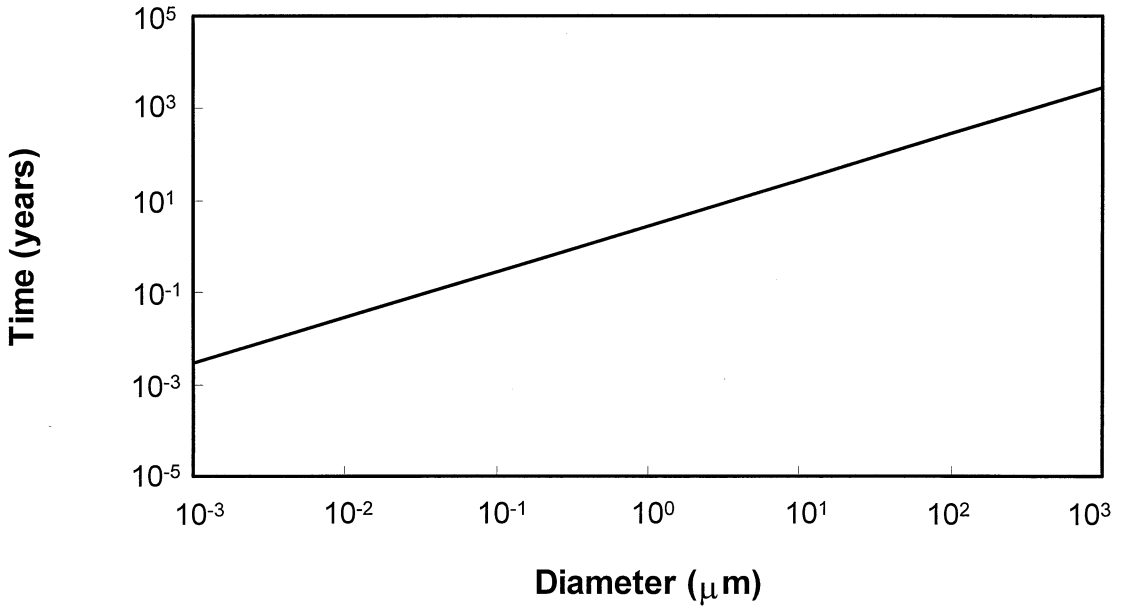

Fig. 9. Particle diameter (μm) vs. time (yr) for the lifetime of an orpiment particle. The orpiment line was calculated by Eqn. 9 with the rate law derived from this study (at pH 7 and DO 7 ppm) and molar volume of 70.51 cm^3/mol.

considered particle diameters, the lifetime of orpiment particle ranges from 8.8×10^4 s to 2.8×10^3 yr at fixed pH and DO concentrations. The range of considered particle diameters is appropriate for natural grain sizes of orpiment.

Commonly, it is assumed that sulfide minerals dissolve faster at low pH values; however, this study shows that the oxidation rates of orpiment increase at higher pH values. If carbonate rock is associated with orpiment and equilibrium with the carbonate rock results in increased pH of solutions, higher As and S concentrations may be released by orpiment oxidation to the natural environment. However, the mobility of As in the natural environment is also commonly controlled by other geochemical reactions such as precipitation/dissolution and adsorption/desorption. The formation of arsenic oxide and salts are not common in the natural environment, except for scorodite ($FeAsO_4 0{\cdot}2H_2O$) (Welch et al., 1988; Bumbla and Keefer, 1994). At near neutral to high pH values, iron, aluminum, and other metals may precipitate in the form of oxides or hydroxides, and these oxides/hydroxides may occur as a sorbent material and retard the As movement in natural environment. A complicating factor to sorption as a process for As removal is that at higher pH values, the surfaces of oxide minerals are commonly negatively charged. Thus, sorption of negatively charged As oxyanions may be minimal and an ineffective means of As removal.

The concentration of dissolved ferric iron and bacteria that may influence the oxidation rates of arsenic sulfide solids have not been evaluated at present. Although ferric iron is an important oxidant at low pH, in near neutral to alkaline pH values, its influence may be reduced because of its low solubility. *Thiobacillus* species are able to oxidize sulfur species in neutral to alkaline pH values; however, they do not dramatically catalyze the rate-limiting steps in pyrite oxidation at pH > 4 (Nicholson et al., 1988).

5. SUMMARY AND CONCLUSIONS

Orpiment oxidation was investigated with a mixed flow reactor at 25 to 40°C with varying pH from 6.8 to 8.2 and DO concentrations of 6.4 to 17.4 ppm. The ratios of total As/S in steady-state conditions are in very good agreement with molar ratios of these elements in the orpiment mineral. The kinetic rate of orpiment oxidation is affected by variable DO concentrations and pH with dependence factors of 0.36 ± 0.09 and 0.47 ± 0.05, respectively. The oxidation rate of orpiment increases with increasing temperature. The activation energy of orpiment oxidation at pH $\sim$7.5 over a temperature range of 25 to 40°C is 59.1 kJ/mol.

Orpiment oxidation by DO resulted in incomplete oxidation for some of the sulfide and As(III) with only partial oxidation to sulfate and As(V). Intermediate sulfur species may be produced during the incomplete orpiment oxidation.

The oxidation of orpiment differs compared with oxidation of As_2S_3(am) in terms of rate law, oxidation rate, and activation energy. Natural orpiment oxidation shows lower dependency on pH than that of As_2S_3(am) and the oxidation rate of natural orpiment is slightly lower, within a factor of 0.05 to 0.72, than that of As_2S_3(am) within the experimental conditions. The activation energy of natural orpiment is approximately 3.5 times larger than that of As_2S_3(am). However, the dominant products from the oxidation of orpiment are similar to As_2S_3(am), where aqueous sulfur species (besides sulfate, sulfite and thiosulfate), As(III), and As(V) are the major products.

Orpiment occurring in mining-impacted environments, such as waste piles or pit lake wall rocks, will oxidize more slowly than pyrite below pH $\sim$8 and will oxidize more rapidly at pH $>$ $\sim$8. Concentrations of As released over time from orpiment will be dependent upon pH and DO conditions, as well as upon the lifetime of the mineral grains. On the basis of our studies, As release during orpiment oxidation increases with pH, and at

higher pH values (>8), the surface charge is negative for most oxide/hydroxide minerals. Thus, at higher pH values, more As will be released during orpiment oxidation, and the natural attenuation of As oxyanions by sorption to mineral surfaces may be diminished.

All of our experiments were conducted with fresh orpiment mineral surfaces. Likely, weathering of the orpiment mineral surface may provide an important control on orpiment mineral reactivity in the natural environment. The oxidation of weathered orpiment was not addressed by this research and provides another opportunity for future studies.

Acknowledgments—Partial support for this study was provided by Placer Dome Inc. The authors gratefully acknowledge Prof. J. Donald Rimstidt and two anonymous reviewers for their constructive comments that contributed to the overall improvement of the article in manuscript. We thank Dr. Mae Gustin for the use of analytical instruments in her laboratory and Angela Paul and Chris Sladek for their assistance in the determination of As species.

Associate editor: J. D. Rimstidt

REFERENCES

Al-Farawati R. and van den Berg C. M. G. (1999) Metal–sulfide complexation in seawater. *Mar. Chem.* **63,** 331–352.

Anthony J. W., Bideaux R. A., Bladh K. W., and Nichols M. C. (1990) *Handbook of Mineralogy*. Mineral Data Publishing.

Barrante J. R. (1998) *Applied Mathematics for Physical Chemistry*. Prentice-Hall.

Birak D. J. and Hawkins R. B. (1985) The geology of the Enfield Bell Mine and the Jerritt Canyon district, Elko county, Nevada. *Geologic Characteristics of Sediment- and Volcanic-Hosted Disseminated Gold Deposits—Search for an Occurrence Model*. In: (ed. W. Tooker), pp. 95–105 Bulletin 1646. U.S. Geological Survey.

Bonham Jr. H. F. (1985) Characteristics of bulk-minable gold-silver deposits in cordilleran and island-arc settings. *Geologic Characteristics of Sediment- and Volcanic-Hosted Disseminated Gold Deposits—Search for an Occurrence Model*. In: (ed. W. Tooker), pp. 71–77 Bulletin 1646. U.S. Geological Survey.

Boyle R. W. and Jonasson I. R. (1972) The geochemistry of arsenic and its use as an indicator element in geochemical prospecting. *J. Geochem. Explor.* **2,** 251–296.

Bumbla D. K. and Keefer R. F. (1994) Arsenic mobilization and bioavailability in soils. *Arsenic in the Environment*. In: (ed. J. O. Nriagu). Wiley, pp. 51–82.

Dickson F. W., Radtke A. S., Weissberg B. G., and Heropoulos C. (1975) Solid solutions of antimony arsenic, and gold in stibnite (Sb_2S_3), orpiment (As_2S_3), and realgar (As_2S_2). *Econ. Geol. Bull. Soc. Econ. Geol.* **70,** 591–594.

Ehrlich H. L. (1963) Bacterial action on orpiment. *Econ. Geol.* **58,** 991–994.

Goldhaber M. B. (1983) Experimental study of metastable sulfur oxyanion formation during pyrite oxidation at pH 6–9 and 30°C. *Am. J. Sci.* **283,** 193–217.

Klein C. and Hurlbut Jr. C. S. (1993) *Manual of Mineralogy*. Wiley.

Lasaga A. C. (1998) *Kinetic Theory in the Earth Sciences*. Princeton University Press.

Lazaro I., Gonzalez I., Cruz R., and Monroy M. G. (1997) Electrochemical study of orpiment (As_2S_3) and realgar (As_2S_2) in acidic medium. *J. Electrochem. Soc.* **144,** 4128–4132.

Lengke M. F. and Tempel R. N. (2001) The kinetic rates of amorphous As_2S_3 oxidation at 25–40°C and initial pH 7.3–9.4. *Geochim. Cosmochim. Acta* **65,** 2241–2255.

Levenspiel O. (1972) *Chemical Reaction Engineering*. Wiley.

McKibben M. A. and Barnes H. L. (1986) Oxidation of pyrite in low temperature acidic solutions: Rate laws and surface textures. *Geochim. Cosmochim. Acta* **50,** 1509–1520.

Moses C. O., Nordstrom D. K., Herman J. S., and Mills A. L. (1987) Aqueous pyrite oxidation by dissolved oxygen and by ferric iron. *Geochim. Cosmochim. Acta* **51,** 1561–1571.

Nagy K. L. and Lasaga A. C. (1992) Dissolution and precipitation kinetics of gibbsite at 80°C and pH 3: The dependence on solution saturation state. *Geochim. Cosmochim. Acta* **56,** 3093–3111.

Nicholson R. V., Gillham R. W., and Reardon E. J. (1988) Pyrite oxidation in carbonate-buffered solution: 1. Experimental kinetics. *Geochim. Cosmochim. Acta* **52,** 1077–1085.

Nicholson R. V., Gillham R. W., and Reardon E. J. (1990) Pyrite oxidation in carbonate-buffered solution: 2. Rate control by oxide coatings. *Geochim. Cosmochim. Acta* **54,** 395–402.

Parkhurst D. L. and Appelo C. A. J. (1999) *User's Guide to PHREEQC—Computer Program for Speciation, Batch Reaction, One-Dimensional-Transport, and Inverse Geochemical Calculations* Water-Resources Investigations Report 99-4259. U.S. Geological Survey.

Shevenell L., Connors K. A., and Henry C. D. (1999) Controls on pit lake water quality at sixteen open-pit mines in Nevada. *Appl. Geochem.* **14,** 669–687.

Turner S. J., Flindell P. A., Hendro D., Hardjana I., Lauricella P. F., Lindsay R. P., Marpaung B., and White G. P. (1994) Sediment-hosted gold mineralisation in the Ratatotok District, North Sulawesi, Indonesia. *J. Geochim. Explor.* **50,** 317–336.

Welch A. H., Lico M. S., and Hughes L. (1988) Arsenic in ground water of the Western United States. *Ground Water* **26,** 333–347.

Williamson M. A. and Rimstidt J. D. (1994) The kinetics and electrochemical rate-determining step of aqueous pyrite oxidation. *Geochim. Cosmochim. Acta* **58,** 5443–5454.